Quantification of intrinsic residual viral replication in treated HIV-infected patients

Christophe Fraser†, Neil M. Ferguson, and Roy M. Anderson

Department of Infectious Disease Epidemiology, Faculty of Medicine, Imperial College of Science, Technology and Medicine, St Mary's Campus, Norfolk Place, Paddington, London W2 1PG, United Kingdom

Edited by Robert May, University of Oxford, Oxford, United Kingdom, and approved October 25, 2001 (received for review June 6, 2001)

The intrinsic rate of viral replication in HIV-infected patients treated with antiretroviral combination therapy is estimated by using a mathematical model of viral dynamics. This intrinsic replication is found to be episodic, varying considerably in quantity between patients (even among those achieving long-term undetectable levels of viremia) and is always reduced by increasing the potency of the antiviral drug regimen. The analysis reveals that even in conditions of perfect patient adherence and drug penetration a substantial level of residual viral replication is expected. The rate of evolution in the viral quasispecies, and thus also the probability of new drug-resistant viral strains being created, is proportional to the total amount of residual viral replication. Under most circumstances, the viral population continues to turn over rapidly during therapy, albeit at a much reduced level.

antiviral therapy | residual replication | mathematical model

Treatment with combinations of antiretroviral compounds that inhibit viral replication is currently the main therapy used to slow progression to serious disease in HIV-infected patients. With the current available drugs, residual viral replication is often observed in otherwise successfully treated patients who show no overt signs of disease (1–4). In this study we quantify the capacity for HIV to replicate in treated patients, using a mathematical model to describe viral dynamics that generates predictions consistent with observed changes in viral load and CD4 abundance seen under therapy (5–10) and long-term trends in HIV pathogenesis (11). Residual replication is shown to be an intrinsic and expected feature of viral dynamics, where its episodic burst-like nature is found to reflect random patterns of host exposure to antigens that drive T cell activation. We quantify viral replication during therapy by using a dynamic measure: the average number of cells newly infected by HIV per day, which is proportional to the probability of emergence of viral resistance *de novo*. A wide range of residual replication rates are shown to be consistent with the apparently successful suppression of viral load, indicating that the viral population can be expected to continue to evolve even under therapy.

Methods

The Model. The model of viral dynamics is defined by eight coupled ordinary differential equations:

$$\frac{dX}{dt} = \Lambda n_a - \mu X - \beta XV$$

$$\frac{dY_L}{dt} = f_L \beta XV - \alpha_L Y_L$$

$$\frac{dY_1}{dt} = (1 - f_L)\beta XV + \alpha_L Y_L - \alpha_1 Y_1$$

$$\frac{dY_2}{dt} = \alpha_1 Y_1 - \alpha_2 Y_2(1 + \sigma Z_2)$$

$$\frac{dV}{dt} = kY_2 - cV$$

$$\frac{dZ_1}{dt} = d(Z^0 - Z_1) + 2pZ_2 - \zeta Y_2 Z_1$$

$$\frac{dZ_2}{dt} = \zeta Y_2 Z_1 - pZ_2$$

$$\frac{dn_a}{dt} = \lambda_a - \alpha_a n_a. \quad [1]$$

These equations describe changes over time in the number X of target cells, Y_L of long-lived infected cells, Y_1 of early-stage infected cells, Y_2 of late-stage infected cells [producing virus and susceptible to cytotoxic T lymphocyte (CTL) lysis], V of free virions, Z_1 of resting HIV-specific CTLs, Z_2 of activated anti-HIV CTLs, and finally n_a of distinct (HIV and non-HIV) antigens that activate CD4 cells. This model has 17 independent parameters, too many to simultaneously estimate by fitting to viral load decay curves, as in refs. 5–8. The parameters and their estimates or assumed values are presented in Table 1. This model builds on earlier related studies (11) and is consistent with long-term observed trends of HIV immunopathogenesis. It provides a realistic description of the viral set-point and its relation to disease progression rates and to the magnitude of the anti-HIV CTL response. Both deterministic and stochastic versions of the model were used in this analysis.

The first departure from the classic models of HIV dynamics (reviewed in ref. 8) is the explicit description of antigen driving the activation of susceptible target $CD4^+$ T cells, and thus driving viral replication. Previous studies of viral treatment have usually described the CD4 pool as a uniform passive target for HIV [although the role of changing activation has been explored (10)]. This is unsatisfactory because HIV replicates primarily in activated cells (12, 13) that make up only a small but changing fraction of the CD4 pool. We choose the simplest possible description of antigen dynamics: antigens eliciting a new CD4 response are encountered by the patient at a Poisson rate λ_a and are then cleared at rate α_a. Each new antigen activates CD4 cells at rate Λ. Because the average number of concurrent antigens is small ($= \lambda_a/\alpha_a$), it is important to model random variations in n_a over time: the long-term variance in n_a is given by its mean (λ_a/α_a). These variations directly change the number of HIV target cells, affecting the efficacy of the whole viral replication cycle.

The second departure from published models is the decomposition of the interaction between CTLs and infected cells into

This paper was submitted directly (Track II) to the PNAS office.

Abbreviation: CTL, cytotoxic T lymphocyte.

†To whom reprint requests should be addressed. E-mail: c.fraser@ic.ac.uk.

The publication costs of this article were defrayed in part by page charge payment. This article must therefore be hereby marked "*advertisement*" in accordance with 18 U.S.C. §1734 solely to indicate this fact.

Table 1. The parameters of the model

Symbol/ equation	Description	Value	Unit	Comments/ref(s).
Λ	Cell activation per antigenic exposure	2.5×10^7	Cells per day	Approx 1:1000 cells activated per day is consistent with pathogenesis (11)
μ	Cell division rate	1	Per day	Activated CD4 cell takes approx. 1 day to divide
β	Viral infectivity	4×10^{-10}	Per virion per cell per day	Derived from R_0 below
f_L	Fraction of infections resulting in a long-lived infected cell	10^{-5}	Per infection	Chosen consistent with known first phase–second phase transitions in viral load decay curves after start of treatment (7)
α_L	Rate of latent infected cell reactivation	0.001	Per day	Fastest observed long-term decay rate (2, 30)
α_1	Rate of progression from cell infection to viral expression and production	1	Per day	(16)
α_2	Death rate of productively infected cell	1	Per day	(16)
σ	Increase in death rate of productively infected cells caused by CTL activity	10^{-5}	Per activated anti-HIV CTL per day	Chosen to match observed frequency of anti-HIV CTLs (15)
k/c	Ratio of free virus to infected cell numbers	1,000	Virions per cell	Conservative estimate based on ref. 32
c	Clearance rate of free virus	25	Per day	Estimated from plasma apheresis experiment (33); precise value unimportant provided fast enough to decouple from model
p	Proliferation rate of activated anti-HIV CTLs	1	Per day	
d	Death rate of anti-HIV CTLs	0.01	Per day	(34)
λ_a	Rate of exposure to new antigens	0.3334	Per day	(11)
α_a	Rate of antigen clearance	0.03334	Per day	Corresponding to an average of 10 concurrent distinct antigens, cleared in 30 days (11)
$\langle R_0 \rangle$	Average basic reproduction number of HIV	100	Number	Higher than lower bound calculated in ref. 19, consistent with pathogenesis (11)
N_{PB}	Factor used to convert figures from 1 ml of peripheral blood to whole body	2.5×10^5	Volume	(6)
ζ	Rate of CTL activation per productive infected cell	(*i*) 1.3334×10^{-8} (*ii*) 1.3334×10^{-9} (*iii*) 1.3334×10^{-10}	Per CTL per infected cell per day	Three example values determine set-point viral load
Steady-state values calculated from the model (for the pretreatment set-point)				
$\hat{V} = \frac{dk}{\zeta c}$	Viral load	(*i*) 7.5×10^8 (*ii*) 7.5×10^9 (*iii*) 7.5×10^{10}	Virions	Gives 3,000, 30,000, and 300,000 virions per ml of peripheral blood, chosen as low, median, and high baseline viral load (28)
$\hat{Y}_2 = \frac{d}{\zeta}$	Number of productively infected cells	(*i*) 7.5×10^5 (*ii*) 7.5×10^6 (*iii*) 7.5×10^7	Cells	
$\hat{X} = \frac{\Lambda \bar{n}_a}{\mu + \beta \hat{V}}$	Number of susceptible cells	(*i*) 1.92×10^8 (*ii*) 6.25×10^7 (*iii*) 8.06×10^6	Cells	
$\hat{Y}_1 = \frac{\beta \hat{X} \hat{Y}_2}{\alpha_1}$	Number of early-stage infected cells	(*i*) 5.77×10^7 (*ii*) 1.88×10^8 (*iii*) 2.42×10^8	Cells	
$\hat{Y}_L = \frac{f_L \beta \hat{X} \hat{Y}_2}{\alpha_L}$	Number of long-lived infected cells	(*i*) 5.77×10^5 (*ii*) 1.88×10^6 (*iii*) 2.42×10^6	Cells	Matches direct estimates (29)
$\hat{Z}_1 + \hat{Z}_2$	Number of anti-HIV CTLs	(*i*) 7.87×10^8 (*ii*) 2.63×10^8 (*iii*) 4.27×10^7	Cells	Matches direct estimates (15)
$\frac{\hat{Z}_2}{\hat{Z}_1 + \hat{Z}_2}$	Percentage of CTLs activated	(*i*) 1% (*ii*) 1% (*iii*) 1%	Percent	
$\frac{\sigma \hat{Z}_2}{1 + \sigma \hat{Z}_2}$	Percentage of infected cells killed by CTLs	(*i*) 98.7% (*ii*) 96.3% (*iii*) 80.9%	Percent	
$\frac{1}{\alpha_1} + \frac{1}{\alpha_2(1 + \sigma \hat{Z}_2)}$	Average lifetime of an infected cell	(*i*) 1.01 (*ii*) 1.04 (*iii*) 1.19	Days	
$\beta \hat{X} \hat{Y}_2$	Number of new cells infected per day	(*i*) 5.77×10^7 (*ii*) 1.88×10^8 (*iii*) 2.42×10^8	Infections per day	To be compared to same quantity calculated after therapy in Fig. 1

(*i*), (*ii*), and (*iii*) refer to parameters for patients with low, median, and high viral loads, respectively.

multiple stages. We model CTL activation by viral antigens as preceding cell division, which occurs at a fixed rate p, and we assume that only activated CTLs can kill infected cells. Dynamically, such a model has several advantages. First, this response explains the large (1000-fold) variation in viral set-point between patients as a result of differences in the ability of CTLs to activate in response to viral antigens, rather than resulting from 1000-fold differences in CTL proliferation or death rates, or even 1000-fold differences in the availability of target cells. The model could be further increased in realism by allowing variation in multiple parameters to explain variations in viral load (as in ref. 14). Second, CTL proliferation is naturally rate limited, with a maximal doubling time of $\ln(2)/p$, independent of other parameters. Third, the observed dynamics are stable, unlike previous models (8) that can exhibit prolonged oscillations in viral and cellular population sizes. Fourth, as seen in Table 1, the model predicts the correct inverse relation between the frequency of anti-HIV CTLs and set-point viral load observed in ref. 15. As highlighted in ref. 16, the division of the infected cell pool into subpopulations of early-stage (previral expression and production) and late-stage infected cells provides a natural explanation for the relative uniformity in infected cell lifetimes inferred from posttherapy decay curves (5, 6).

The equations are integrated in fixed time steps of $\Delta t = 0.01$ day. For the stochastic model, n_a is increased in each time step by a Poisson deviate of mean $\lambda_a \Delta t$, and reduced by binomial deviate with probability $\alpha_a \Delta t$ and sample size n_a. For the deterministic model n_a is fixed $= \lambda_a/\alpha_a$. The other equations are integrated by using a fourth-order Runge–Kutta algorithm, assuming fixed n_a over the interval (17).

The Basic Reproduction Number. The basic reproduction number is the number of new cells that an infected cell infects before it dies, in the absence of density-dependent constraints (8). For this model, it is approximately given by

$$R_0 = \frac{\Lambda n_a \beta k}{\mu \alpha_2 c}. \qquad [2]$$

It is a function of the number of distinct antigens n_a and so fluctuates over time.

The average value of R_0 in the stochastic model, denoted $<R_0>$, coincides with the value of R_0 in the deterministic model, and is given by

$$\langle R_0 \rangle = \frac{\beta k X_0}{\alpha_2 c}, \qquad [3]$$

where $X_0 = \Lambda \lambda_a/\alpha_a$ is the average number of susceptible target cells in the absence of HIV infection.

Steady States of the Deterministic Model. The deterministic model has three equilibria. In the equations below, we approximate $Z^0 \approx 0$. The uninfected equilibrium is given by

$$X^{(1)} = X_0 \quad Y_1^{(1)} = 0 \quad Y_2^{(1)} = 0 \quad Z_2^{(1)} = 0. \qquad [4]$$

There are two infected equilibria. The first has no sustained CTL response, and is given by

$$\begin{aligned} X^{(2)} &= \frac{X_0}{\langle R_0 \rangle} \quad Y_1^{(2)} = \frac{\mu X_0}{\alpha_1}\left(1 - \frac{1}{\langle R_0 \rangle}\right) \\ Y_2^{(2)} &= \frac{\mu X_0}{\alpha_2}\left(1 - \frac{1}{\langle R_0 \rangle}\right) \quad Z_2^{(2)} = 0. \end{aligned} \qquad [5]$$

The second infected equilibrium is associated with a stable effective anti-HIV CTL response, and is given by

$$\begin{aligned} X^{(3)} &= \frac{X_0}{R_0^{\mathrm{CTL}}} \quad Y_1^{(3)} = \frac{\mu X_0}{\alpha_1}\left(1 - \frac{1}{R_0^{\mathrm{CTL}}}\right) \\ Y_2^{(3)} &= \frac{\xi}{d} \quad Z_2^{(3)} = \frac{1}{\sigma}\left(\frac{\langle R_0 \rangle}{R_0^{\mathrm{CTL}}} - 1\right). \end{aligned} \qquad [6]$$

In the above, we define R_0^{CTL} to be the CTL-restricted reproduction number, as the number of secondary infections caused by an infected cell before it dies, in the presence of a mature CTL response. It is defined by analogy with R_0 and is given by

$$R_0^{\mathrm{CTL}} = 1 + \frac{\beta k d}{c d \zeta}. \qquad [7]$$

For all equilibria, the remaining densities are given by

$$Y_{\mathrm{L}}^{(*)} = \frac{f_{\mathrm{L}} \alpha_1}{\alpha_{\mathrm{L}}} Y_1^{(*)} \quad V^{(*)} = \frac{k}{c} Y_2^{(*)} \quad Z_1^{(*)} = \frac{d}{p} Z_2^{(*)}. \qquad [8]$$

The uninfected steady state, defined in Eq. **4**, is stable if and only if $\langle R_0 \rangle < 1$. The CTL-free infected steady state, defined in Eq. **5**, is stable if and only if $R_0^{\mathrm{CTL}} > \langle R_0 \rangle > 1$. The CTL-restricted steady state, defined in Eq. **6**, is stable if and only if $\langle R_0 \rangle > R_0^{\mathrm{CTL}} > 1$. The parameters that define the boundaries between these stable states are threshold values.

Calculation of the Threshold Treatment Efficacies. For the parameters we use (defined in Table 1), before antiviral treatment, the patients are in the CTL-restricted steady-state defined by Eq. **6**. The effect of antiviral therapy is to reduce the ratio $\beta k/c$ to $(\beta k/c)(1 - \varepsilon)$, where ε is the treatment efficacy (7, 18); the thresholds separating equilibrium **6** from **5** and **5** from **4** are crossed sequentially with increasing ε. The threshold efficacies are given by

$$\varepsilon_1 = 1 - \frac{1}{\langle R_0 \rangle + 1 - R_0^{\mathrm{CTL}}} \qquad [9]$$

for the first crossing and

$$\varepsilon_2 = 1 - \frac{1}{\langle R_0 \rangle} \qquad [10]$$

for the second.

The third threshold discussed arises from the reduction in the replenishment of the resting cell pool attributable to activated CD4 cells being destroyed as a result of HIV replication. The replenishment rate is proportional to the number of susceptible cells $X^{(*)}$, and thus it increases as treatment efficacy increases. If p_S is the probability that an activated cell will successfully divide, then the threshold treatment efficacy is

$$\varepsilon_3 = \min\left(1 - \frac{2p_S}{\langle R_0 \rangle}; 1 - \frac{2p_S - 1}{R_0^{\mathrm{CTL}} - 1}\right). \qquad [11]$$

Stochastic effects do not remove, but rather blur, these threshold effects.

Results

The key quantity that captures the capacity for viral replication within the patient is the basic reproduction number, R_0, defined as the average number of secondary cell infections caused by the introduction of a single infected cell into a susceptible person (8, 19). The definition and derivation of R_0, as well as the underlying

biological assumptions incorporated into a mathematical model of HIV replication, are presented in *Methods*. An important feature of this model is that R_0 is not fixed, but varies as a function of the rate of activation of CD4 cells; this in turn reflects the temporal pattern of exposure to HIV and non-HIV antigens. The extent to which antiretroviral therapy inhibits viral replication is simply the factor by which it reduces the magnitude of R_0 (7, 18), thus providing both a precise definition for treatment efficacy and a measurement tool.

The long-term outcome of therapy depends crucially on the magnitude of the reduced value of R_0 because this relates to the net rate of evolution of the virus. The dependence between the magnitude of R_0 (determined by treatment efficacy) and the long-term outcome of treatment is predicted to be more complex than suggested by previous theoretical studies of HIV dynamics (20), in accord with observed patterns (9). In *Methods*, we describe how our model can be formulated as deterministic or stochastic, corresponding respectively to a fixed or a randomly fluctuating level of antigenic stimulation and subsequent T cell activation. We start by describing the deterministic model because it is simpler: antigenic stimulation, T cell activation, and thus R_0 are all constant over time. We observe four qualitatively different outcomes to antiviral therapy, separated by three threshold values of treatment efficacy (derived in *Methods*). The short-term effect is always a reduction in viral load. The distinct dynamical regimes are as follows:

1. The short-term effect of low-efficacy treatment is to reduce the number of anti-HIV CTLs in circulation caused by a transient reduction in viral load. In the long term, viral load returns to its pretreatment value, whereas the number of CTLs remains reduced. The long-term effect of therapy is only a modest reduction in viral load because of the tradeoff between drug action and reduced CTL action.

2. As treatment efficacy is increased and R_0 is reduced, a CTL stimulation threshold is crossed and the efficacy of the CTL response declines because of lower rates of activation caused by the reduced viral population (21).

3. At a second threshold, the probability that a CD4 cell can successfully divide without being either infected or suffering activation-related death reaches 0.5. Above this value therapy causes a change in viral load to a new and lower set-point but no continuing decay in viral load. However, the long-term depletion of CD4 cells is reversed (11), so overall this scenario represents a discordant response to therapy.

4. The third threshold is achieved when R_0 falls below unity in value: below this value viral replication becomes unsustainable and a rapid biphasic decay in viral load is observed (7).

The order on which the thresholds are crossed depends on the parameter values, but is always either 1–2-3–4 or 1–3-2–4.

The effect of random variations in the number of antigens that are activating the CD4 cell pool is to cause R_0, and concomitantly viral load, to fluctuate. When treatment efficacy is close to a threshold value, this introduces a degree of intermittency to the viral dynamics as the system bounces below and above the threshold, as seen in the viral load decay curves plotted in Fig. 1. Random antigenic exposures can therefore temporarily shift the patient back and forth between the states of viral decay and viral growth. It is thus a prediction of the model that short episodes of sustained viral replication are an intrinsic part of the dynamics of antiretroviral treatment. The duration of these intermittent episodes is determined by the average time taken to clear a typical antigen (given by $1/\alpha_a$ in the model: see *Methods*). The magnitude and frequency of these episodes is predicted to decrease with increasing treatment efficacy (Fig. 1), as clinically observed.

The model was further used to quantify the amount of residual replication expected in patients where treatment efficacy is on average sufficient to render viral replication unsustainable ($R_0 <$ 1 on average). Two measures were estimated: one for the first 50 days of treatment, and one for the subsequent 250 days. This approach was adopted because a high rate of target cell infection is expected in the early parts of treatment when viral loads are still high, and a low rate once treatment effectively suppresses viral load. The measure of viral replication used was the average number of cells infected by HIV per day, as plotted in Fig. 1, as a function of the value of the average posttherapy R_0. Because the average pretherapy R_0 is fixed in the simulation, posttherapy R_0 and treatment efficacy are interchangeable: the lower R_0, the higher the efficacy. The simulation was repeated 1,000 times for 100 different values of R_0, separately for patients with high, median, or low set-point viral loads (as defined in Table 1). Comparative values are given for the deterministic model to illustrate the effect of intermittency on residual replication. The predicted fraction of patients achieving undetectable levels of virus after 50 days and after 24 weeks [gauged at $<$5 copies per ml of peripheral blood, in line with current ultrasensitive assays (7)], are also plotted in Fig. 1.

The analysis shows that for high-efficacy drug regimens, there is considerably more residual replication in the early part of treatment. For marginally effective treatments (R_0 close to 1), antigen-driven intermittency was found to increase long-term residual replication substantially above that predicted by the deterministic model, up to levels equivalent to the first 50 days of treatment, and the number of patients failing to reach undetectable levels of virus dropped accordingly (independent of other factors such as poor compliance or the emergence of viral resistance to treatment). Outside this zone, the outcomes of the simulation are centered on the prediction of the deterministic model, thus randomly varying antigenic exposure does not in general predict more residual replication to occur than the model where this is constant. In identical simulations, a minimum 2-fold variation in the average number of cells newly infected per day was found.

The measure used was approximately equal to the number of new mutations generated in the viral population, and thus also to the probability of emergence of *de novo* drug resistance (8, 22, 23). This probability is expected to relate to the likelihood of treatment failure in the long term (20). The variation reflects the randomness of antigenic encounters in simulated patients with identical parameters. A millionfold variation in viral replication was observed in the range $0.1 < R_0 < 1$ (corresponding to 0.9% variation in treatment efficacy). Even when 100% of the patients are predicted to reach undetectable viral loads ($R_0 < \approx 0.5$), more than a hundredfold variation in residual viral replication was observed. The degree of residual replication was found to be intrinsically variable, but is always reduced by increasing treatment efficacy.

Discussion

Persistent viral replication, even at low levels, compromises the long-term success of therapy by providing opportunities for the evolution of drug-resistant variants of the virus (the net rate of evolution is directly proportional to the net rate of viral replication) and concomitant treatment failure. There are many factors that can cause residual replication in treated HIV-infected patients (24). Poor adherence of patients to treatment protocols has been shown to be predictive of drug failure (25). Cellular reservoirs or physiological compartments (such as the central nervous system) where drug penetration is poor have also been implicated (24). Whereas the reality of *in vivo* treatment is multifactorial, the use of a mathematical model allows us to separately analyze and dissect these factors, performing a "virtual experiment" to estimate how much residual replication is intrinsic to the stochastic dynamics of viral replication and antigenic exposure. The estimates are subject to the caveat that

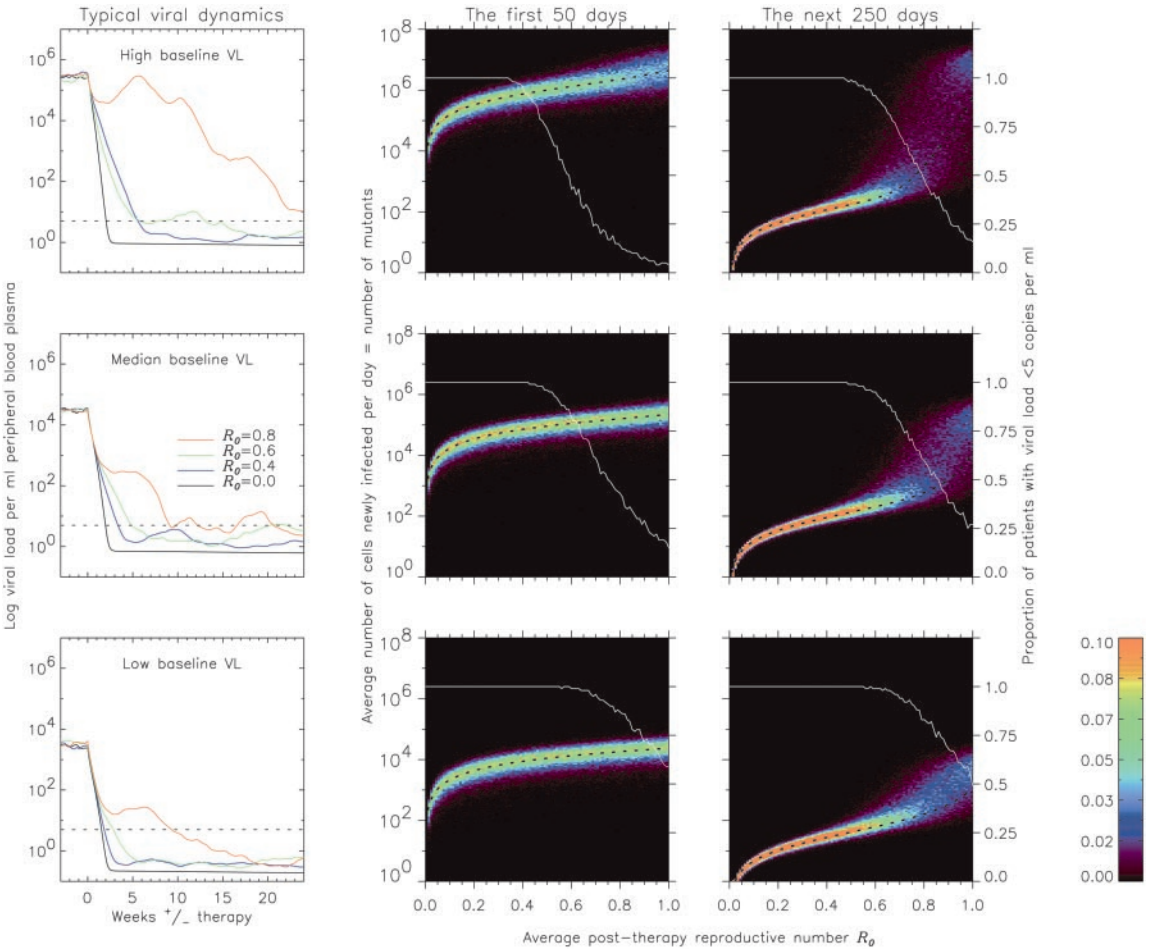

Fig. 1. Residual viral replication in treated HIV-positive patients. The figure illustrates results from the simulation for three sets of patients with high, median, and low set-point viral loads (300,000, 30,000, and 3,000 copies per ml in the *Top, Middle,* and *Bottom* graphs, respectively). The graphs to the *Left* show typical outcomes for a range of different treatment efficacies, as measured by the posttherapy average basic reproduction number R_0. The dashed line indicates a limit of detection of 5 copies per ml. The graphs in the *Center* and *Right* columns illustrate the outcome of 1,000 separate simulations for 100 values of R_0. For each simulation the average number of residual infections is recorded during the first 50 days (*Center*) and the subsequent 250 days (*Right*). The color of the graph illustrates the relative frequency of each outcome, as scaled by the color bar on the right. The dotted black line is the prediction calculated from the deterministic model in which antigenic exposure is assumed constant rather than random. The white line on these graphs is the fraction of the 1,000 simulated patients that reach levels of virus <5 copies per ml, after 50 days in the *Center* graphs, and after 24 weeks in the graphs to the *Right*.

they extrapolate information from peripheral blood measurements to the whole body, whereas there is an additional contribution to viral decay and diversity from virus attached to follicular dendritic cells in lymphatic tissues (26).

The mathematical model is founded on a substantial experimental, observational, and theoretical literature (recently reviewed in ref. 8). The model captures both the role of antigenic exposure in regulating viral replication by limiting the number of available target cells for HIV to those that are in the dividing stage (12), and the impact of an active CTL response (27). It predicts a pattern of intermittency in viral replication during therapy, and thus offers an explanation for the episodic nature of viral replication in patients known to adhere well to treatment regimens (4). The model also helps explain the wide variations in pretreatment viral load seen between patients (28). The description of a multistage model (i.e., resting and activated HIV antigen-specific cells) to describe the anti-HIV CTL response generates predictions consistent both with long-term trends in HIV pathogenesis (11) and with the relative constancy in infected cell lifetimes (16).

Several recent studies have found evidence for active viral transcription in patients where viral load is successfully suppressed (1–3). Such residual replication is thought to replenish stocks of long-lived infected CD4 cells (4), which are held responsible for long-term viral persistence in infected patients (29, 30). The current study shows unambiguously that a substantial amount of residual viral replication is an intrinsic feature of HIV dynamics during antiretroviral therapy, and that the viral population continues to turn over rapidly, albeit at a much-reduced net rate. Even when currently undetectable levels of virus are reached, there remains scope to reduce residual replication by intensifying the treatment [e.g., five-drug regimens (7)]. Intensifying treatment by using drugs with better pharmacodynamic properties (i.e., a greater ability to suppress viral replication and longer half-lives) and attempting to minimize poor patient adherence by education and counseling is essential to reduce current rates of treatment failure (31). However, a recent re-appraisal of pharmacodynamic measures of drug efficacy indicates that complete blocking of viral replication by the combinations of the currently available drugs is more difficult than previously thought (18).

C.F. and R.M.A. thank the Wellcome Trust for funding and N.M.F. thanks the Royal Society.

1. Furtado, M. R., Callaway, D. S., Phair, J. P., Kunstman, K. J., Stanton, J. L., Macken, C. A., Perelson, A. S. & Wolinsky, S. M. (1999) *N. Engl. J. Med.* **340,** 1614–1622.
2. Zhang, L., Ramratnam, B., Tenner-Racz, K., He, Y., Vesanen, M., Lewin, S., Talal, A., Racz, P., Perelson, A. S., Korber, B. T., *et al*. (1999) *N. Engl. J. Med.* **340,** 1605–1613.
3. Sharkey, M. E., Teo, I., Greenough, T., Sharova, N., Luzuriaga, K., Sullivan, J. L., Bucy, R. P., Kostrikis, L. G., Haase, A., Veryard, C., *et al*. (2000) *Nat. Med.* **6,** 76–81.
4. Ramratnam, B., Mittler, J. E., Zhang, L. Q., Boden, D., Hurley, A., Fang, F., Macken, C. A., Perelson, A. S., Markowitz, M. & Ho, D. D. (2000) *Nat. Med.* **6,** 82–85.
5. Wei, X. P., Ghosh, S. K., Taylor, M. E., Johnson, V. A., Emini, E. A., Deutsch, P., Lifson, J. D., Bonhoeffer, S., Nowak, M. A., Hahn, B. H., *et al*. (1995) *Nature (London)* **373,** 117–122.
6. Ho, D. D., Neumann, A. U., Perelson, A. S., Chen, W., Leonard, J. M. & Markowitz, M. (1995) *Nature (London)* **373,** 123–126.
7. Ferguson, N. M., de Wolf, F., Ghani, A. C., Fraser, C., Donnelly, C. A., Reiss, P., Lange, J. M. A., Danner, S. A., Garnett, G. P., Goudsmit, J. & Anderson, R. M. (1999) *Proc. Natl. Acad. Sci. USA* **96,** 15167–15172.
8. Nowak, M. A. & May, R. M. (2000) *Virus Dynamics: Mathematical Principles of Immunology and Virology* (Oxford Univ. Press, Oxford).
9. Kaufmann, D., Pantaleo, G., Sudre, P. & Telenti, A. (1998) *Lancet* **351,** 723–724.
10. Grossman, Z., Polis, M., Feinberg, M. B., Levi, I., Jankelevich, S., Yarchoan, R., Boon, J., de Wolf, F., Lange, J. M. A., Goudsmit, J., *et al*. (1999) *Nat. Med.* **5,** 1099–1104.
11. Fraser, C., Ferguson, N. M., de Wolf, F. & Anderson, R. M. (2001) *Proc. R. Soc. London Ser. B* **268,** 2085–2095.
12. Stevenson, M., Stanwick, T. L., Dempsey, M. P. & Lamonica, C. A. (1990) *EMBO J.* **9,** 1551–1560.
13. Orendi, J. M., Bloem, A. C., Borleffs, J. C. C., Wijnholds, F. J., deVos, N. M., Nottet, H. S. L. M., Visser, M. R., Snippe, H., Verhoef, J. & Boucher, C. A. B. (1998) *J. Infect. Dis.* **178,** 1279–1287.
14. Muller, V., Maree, A. F. M. & De Boer, R. J. (2001) *Proc. R. Soc. London Ser. B* **268,** 235–242.
15. Ogg, G. S., Jin, X., Bonhoeffer, S., Dunbar, P. R., Nowak, M. A., Monard, S., Segal, J. P., Cao, Y. Z., Rowland-Jones, S. L., Cerundolo, V., *et al*. (1998) *Science* **279,** 2103–2106.
16. Klenerman, P., Phillips, R. E., Rinaldo, C. R., Wahl, L. M., Ogg, G., May, R. M., McMichael, A. J. & Nowak, M. A. (1996) *Proc. Natl. Acad. Sci. USA* **93,** 15323–15328.
17. Press, W. H., Teukolsky, S. A., Vetterling, W. T. & Flannery, B. P. (1992) *Numerical Recipes in C: The Art of Scientific Computing* (Cambridge Univ. Press, Cambridge, U.K.).
18. Ferguson, N. M., Fraser, C. & Anderson, R. M. (2001) *Trends Pharmacol. Sci.* **22,** 97–100.
19. Little, S. J., McLean, A. R., Spina, C. A., Richman, D. D. & Havlir, D. V. (1999) *J. Exp. Med.* **190,** 841–850.
20. Bonhoeffer, S., May, R. M., Shaw, G. M. & Nowak, M. A. (1997) *Proc. Natl. Acad. Sci. USA* **94,** 6971–6976.
21. Wodarz, D., May, R. M. & Nowak, M. A. (2000) *Int. Immunol.* **12,** 467–477.
22. Nowak, M. A., Anderson, R. M., McLean, A. R., Wolfs, T. F. W., Goudsmit, J. & May, R. M. (1991) *Science* **254,** 963–969.
23. Ribeiro, R. M. & Bonhoeffer, S. (2000) *Proc. Natl. Acad. Sci. USA* **97,** 7681–7686.
24. Deeks, S. G. (2000) *Clin. Infect. Dis.* **30,** S177–S184.
25. Paterson, D. L., Swindells, S., Mohr, J., Brester, M., Vergis, E. N., Squier, C., Wagener, M. M. & Singh, N. (2000) *Ann. Intern. Med.* **133,** 21–30.
26. Hlavacek, W. S., Stilianakis, N. I., Notermans, D. W., Danner, S. A. & Perelson, A. S. (2000) *Proc. Natl. Acad. Sci. USA* **97,** 10966–10971. (First Published September 19, 2000; 10.1073/pnas.190065897)
27. Jin, X., Bauer, D. E., Tuttleton, S. E., Lewin, S., Gettie, A., Blanchard, J., Irwin, C. E., Safrit, J. T., Mittler, J., Weinberger, L., *et al*. (1999) *J. Exp. Med.* **189,** 991–998.
28. Mellors, J. W., Rinaldo, C. R., Gupta, P., White, R. M., Todd, J. A. & Kingsley, L. A. (1996) *Science* **272,** 1167–1170.
29. Chun, T. W., Carruth, L., Finzi, D., Shen, X. F., DiGiuseppe, J. A., Taylor, H., Hermankova, M., Chadwick, K., Margolick, J., Quinn, T. C., *et al*. (1997) *Nature (London)* **387,** 183–188.
30. Finzi, D., Blankson, J., Siliciano, J. D., Margolick, J., Chadwick, K., Pierson, T., Smith, K., Lisziewicz, J., Lori, F., Flexner, C., *et al*. (1999) *Nat. Med.* **5,** 512–517.
31. Mocroft, A., Miller, V., Chiesi, A., Blaxhult, A., Katlama, C., Clotet, B., Barton, S. & Lundgren, J. D. (2000) *Antiviral Ther.* **5,** 107–112.
32. Hockett, R. D., Kilby, J. M., Derdeyn, C. A., Saag, M. S., Sillers, M., Squires, K., Chiz, S., Nowak, M. A., Shaw, G. M. & Bucy, R. P. (1999) *J. Exp. Med.* **189,** 1545–1554.
33. Ramratnam, B., Bonhoeffer, S., Binley, J., Hurley, A., Zhang, L. Q., Mittler, J. E., Markowitz, M., Moore, J. P., Perelson, A. S. & Ho, D. D. (1999) *Lancet* **354,** 1782–1785.
34. Ogg, G. S., Jin, X., Bonhoeffer, S., Moss, P., Nowak, M. A., Monard, S., Segal, J. P., Cao, Y., Rowland-Jones, S. L., Hurley, A., *et al*. (1999) *J. Virol.* **73,** 797–800.